

# 101711ERSIDEBANDSPECTRAFOR IONS IN A LINEAR TRAP<sup>1</sup>

John D. Prestage, Robert L. Tjoelker, G. 101111 Dick, and Lute Maleki

California Institute of Technology  
Jet Propulsion Laboratory  
4800 Oak Grove Drive  
Pasadena, CA 91109

## Abstract

We describe a spectroscopic measurement of the temperature and linear density of  $\text{Hg}^+$  ions held in a linear ion trap (LIT). The inferred temperature and number result from analysis of sidebands on the 40.5 GHz resonance line. The temperature of the ion cloud is determined by the Doppler broadened line when microwave radiation is propagated along the axis of the LIT. When propagation is perpendicular to the trap axis the microwave sidebands are displaced from the trap secular frequency by an amount dependent upon the ion cloud size and temperature. A Monte-Carlo simulation of the ion trajectories inside the cloud is used to model the position of these sidebands for a given cloud temperature and a comparison with measured sideband position is used to determine ion number.

## Introduction

One of the largest frequency offsets in lamp based buffer gas cooled Mercury ion frequency standards is the second order Doppler shift from the thermal and micro-motion of the ions within the trap [1,2]. At room temperature with  $\text{Hg}^+$  ions in a LIT this shift is  $(1+2/3)3k_B T / (2mc^2) = 3.5 \times 10^{-13}$  for a small cloud where space charge screening of the time averaged trapping field is negligible. In this case a measurement of ion cloud temperature accurate to 10% would yield a room temperature Hg clock with accuracy at few parts in  $10^{14}$ , approaching that of the best primary Cesium

standards currently in operation. This paper describes temperature measurements and ion number determination for ion clouds held in a linear ion trap. Such measurements are necessary to assess clock frequency offset from the 2nd order Doppler shift and to determine clock accuracy [3]. Knowledge of cloud size and temperature also serves as a useful diagnostic of ion trap operation.

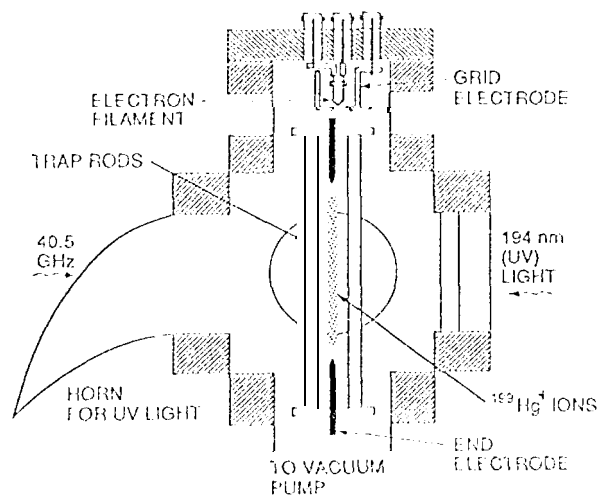


Figure 1: Linear ion trap residing in its high vacuum enclosure. Stale selection light from the  $^{201}\text{Hg}$  discharge lamp is focused onto the central 1/3 of the ion cloud. Atomic fluorescence is collected normal to the page.

<sup>1</sup>This work represents one phase of research carried out at the Jet Propulsion Laboratory, California Institute of Technology, under contract to the National Aeronautics and Space Administration.

Figure 1 shows the present  $I, I'$  configuration as used in clock operation [4]. Ions are confined in the cylindrical cloud up to 75 mm in length by a few mm in diameter. An ion's thermal motion inside the cloud will lead to a high frequency secular motion corresponding to transit across the few mm cloud diameter and a much lower frequency corresponding to axial motion along the approximately 75 mm long cloud. When there are only a few ions in the trap the resultant forces on the ions are predominately from the trapping fields. The transverse motion is then harmonic and all ions undergo motion at the secular frequency of the trap. As the 40.5 GHz radiation propagates radially through the cloud an ion's motion in the trap will modulate the phase of the microwaves. This results in sidebands on the atomic absorption spectrum of  $\pm$  the 40.5 GHz carrier by the trap secular frequency and its harmonics. As more ions are added to the trap the cumulative effect of the trapped charges begins to shield the time averaged trapping fields from the interior of the ion cloud. Ions moving inside the cloud will no longer feel the harmonic trapping well and the result is a broadened and downshifted Doppler sideband spectrum. We have computed the spectrum of microwave power seen by an ion moving through the cloud by a Monte-Carlo sampling of ion trajectories and the resulting phase variation. For a fixed cloud temperature the Doppler sideband shifts downward monotonically with increasing number of trapped ions. Once the ion temperature has been measured the cloud size is determined by adjusting ion number until the simulated and measured sideband frequencies match.

### Ion Temperature Measurement

We measure ion temperature spectroscopically by propagating the 40.5 GHz resonance radiation along the 75 mm long axis of the ion cloud. In this configuration ion confinement is 10 times the wavelength of the 7.5 mm resonance radiation and the Doppler width of the 40.5 GHz absorption line is used to determine the cloud temperature [5]. Because the 50 mini-gauss bias field is parallel to this axis of the trap and hence perpendicular to the oscillating magnetic field of the microwave radiation, the allowed transitions obey  $\Delta m_j = \pm 1$ . These transitions are from the  $F=0, m_j=0$  state to the  $F=1, m_j=\pm 1$  Zeeman states. Figure 2 shows the Doppler broadened microwave lines obtained by propagating microwaves along this direction. The width of the microwave transition is  $\delta\nu = 2(\nu/c)(2k_B T \ln 2/m)^{1/2} = 2.056 T^{1/2}$  kHz [6], where  $T$  is temperature in Kelvin. The 46 kHz wide spectral

lines in Fig. 2 indicate an ion cloud temperature of 500 K. By use of this technique we have measured ion cloud temperature variations with helium buffer gas pressure. As shown in Figure 3 the ion temperature varies from 2610 K at  $2 \times 10^{-8}$  Torr (uncorrected) to 480 K at  $7 \times 10^{-6}$  Torr (uncorrected). For the clouds used in our clock measurements Helium pressures above  $2 \times 10^{-6}$  Torr (uncorrected) are necessary for minimum temperatures.

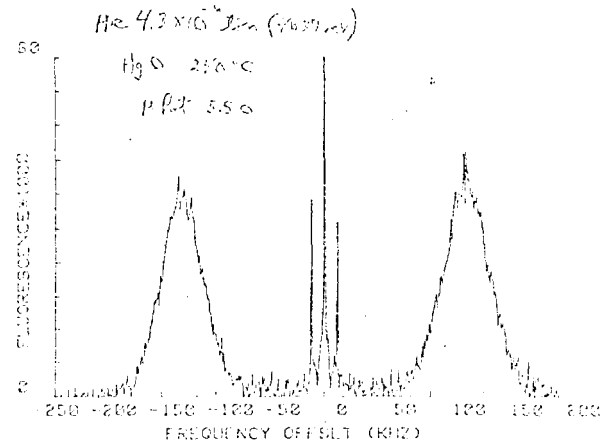


Figure 2: The Doppler broadened Zeeman hyperfine transitions  $F=0, m_j=0$  to  $F=1, m_j=\pm 1$  which are used to determine the  $Hg^+$  temperature. For this measurement the 40.5 GHz radiation passed axially through the 75 mm long cloud.

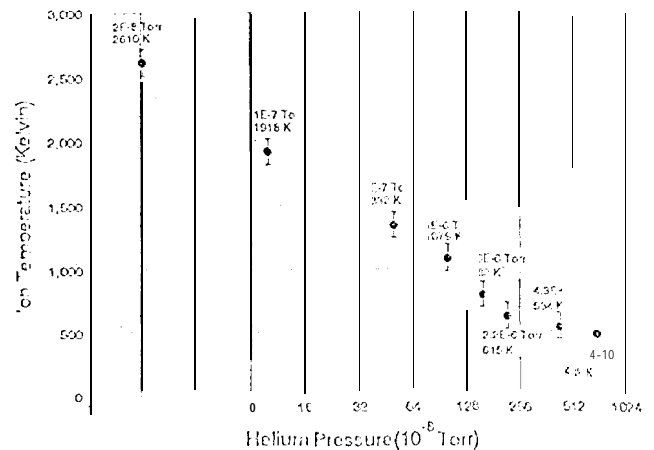


Figure 3:  $Hg^+$  cloud temperature vs helium buffer gas pressure as determined from the doppler width of the 40.5 GHz transition.

### Transverse Microwave Excitation of Ion Cloud

By propagating the 40.5 GHz resonance radiation perpendicular to the long axis of the ion cloud we can investigate the absorption sidebands which stem from the high frequency secular ion motion across the cloud diameter. The measured resonance structure is shown in Figure 4 (a) and (b). In Fig. 4(a) the helium pressure is  $5 \times 10^{-8}$  Torr (uncorrected) so ion temperature is over 2000 K. The calculated secular frequency at the

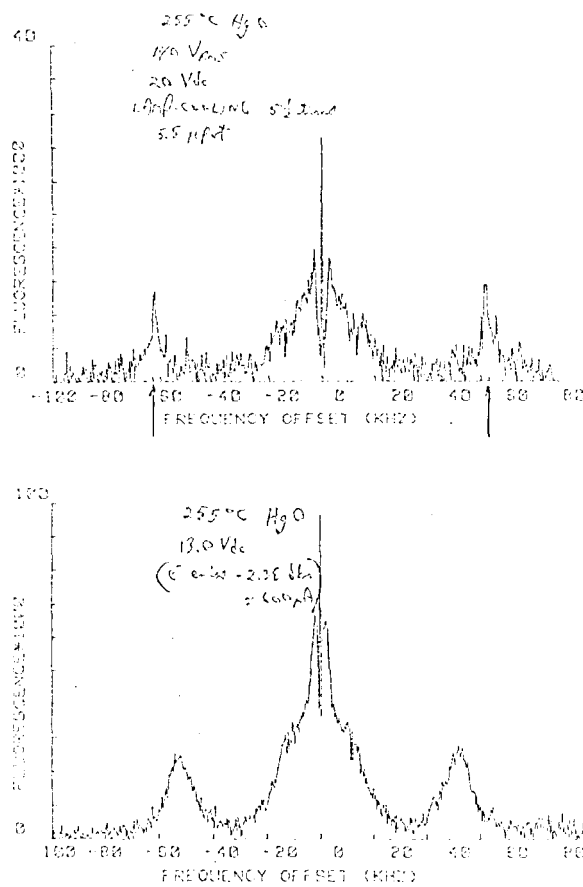


Figure 4: Sideband spectra obtained by transverse microwave illumination of the ion cloud as shown in Fig. 1. (a) Low helium buffer pressure and resulting ion temperature over 2000 K. Sidebands show very little shift from the 62 kHz trap secular frequency. (b) Sidebands shift by 10 kHz as the helium pressure is increased and ion temperature falls to 650 K.

operating rf voltage level (140 Volts rms @ 853 kHz) is 62 kHz and is in good agreement with the frequency of the transverse sidebands. This indicates low ion density since there is no significant screening of the trapping fields by the ion space charge. By contrast Fig. 4(b) shows that the sidebands have shifted closer to the 40.5 GHz carrier by about 10 kHz as the helium pressure was increased to  $2 \times 10^{-6}$  Torr (uncorrected). The signal size has also quadrupled since many more ions are trapped under these conditions.

### Monte-Carlo calculation of Sideband Frequencies

The approach used in predicting the frequency of the secular sidebands as described above is to determine the microwave frequency spectrum seen by an ion inside the cloud [7]. A spherical wavefront is incident on the ion cloud from a distance  $R_0$ . The magnetic field seen by an ion at position  $r$  at time  $t$  is

$$B(r,t) = B_0 \exp[i(k_{\mu w} r - \omega t)] / (k_{\mu w} r)$$

where  $k_{\mu w} = 2\pi/\lambda_{\mu w}$  and  $\lambda_{\mu w}$  is the wavelength of the microwave radiation,  $\approx 7.5$  mm. The ions are in thermal motion inside the cloud so that  $r = r(t)$  and the spherical wave is modulated by the individual ion motions. This motion is determined by the velocity distribution and the shape of the ion cloud. The long thin cloud leads to microwave modulation frequencies of order  $v_{mp}/D$  and  $v_{mp}/L$ , where  $v_{mp}$  is the most probable velocity for the ions at temperature  $T$ ,  $D$  is the cloud diameter and  $L$  is the cloud length. The power spectral density of the 40.5 GHz radiation as seen by the ensemble of confined moving ions is related to the autocorrelation function of the microwave magnetic field through the cosine transform (Wiener-Khinchine Theorem)

$$P(\omega) = \int d\tau \psi(\tau) \cos \omega \tau$$

where  $\psi(\tau)$  is the autocorrelation function

$$\psi(\tau) = B_0^2 \text{Re} \{ \exp(-ik_{\mu w}(r(\tau) - r(0))) / (k_{\mu w}^2 r(0)r(\tau)) \}$$

The averaging is to be carried out over the ionic trajectories through the cloud. To generate this average a set of initial conditions consistent with the velocity and position distribution functions is chosen with a trajectory being generated through the potentials seen inside the cloud. Ignoring collisions, an ion moves in response to the space charge potential of the other ions and the harmonic trap potential. The

starting point is calculation of the density profile for a given number of ions at temperature  $T$  in a cylindrically symmetric harmonic trapping well of secular frequency  $\omega$  [8]. The ion cloud is assumed to be of uniform linear density  $U_p$  to the ends of the trap.

### Boltzmann Density Profile

We assume that the ion cloud is in thermal equilibrium at temperature ' $T$ ' so that the ion number density  $n(\rho)$  satisfies a Boltzmann distribution [7]

$$n(\rho) = n(0) \exp[-\Phi_{\text{total}}(\rho) / k_B T]$$

where  $\Phi_{\text{total}}(\rho) = m\omega^2 \rho^2 / 2 + q\phi_{\text{sc}}(\rho)$  is the sum of the trapping field and ion cloud space charge potential energies, respectively and  $\rho$  is the radial distance from the trap axis. Poisson's equation ( $\nabla^2 \phi_{\text{sc}}(\rho) = -qn(\rho) / \epsilon_0$ ) leads to a non-linear differential equation for  $n(\rho)$

$$n'' + n' / \rho - (n')^2 / n + n(n_0 - n) / (n_0 \lambda_D^2) = 0$$

where  $n_0 = 2\epsilon_0 m \omega^2 / q^2$  is the pseudocharge or saturation density for ions in the trap. The Debye length  $\lambda_D = \sqrt{\epsilon_0 k_B T / (110 q^2 n)} = \sqrt{k_B T / (2m\omega^2)}$  is a measure of the penetration length of the time averaged trapping fields into the ion cloud interior. This equation is numerically solved (subject to  $2\pi \int \rho n(\rho) d\rho = N/l$ ) via Runge-Kutta methods to give density profiles as shown in Figure 5. The 62 kHz trap secular frequency leads to a saturation density of 34,840 ions per mm<sup>3</sup> which at 500 K ion temperature gives a Debye length 0.26 mm. If mill  $4\pi n_0 a^3 / 3 = 1$  we estimate an inter-ion spacing  $a = 19 \mu\text{m}$  at saturation density. The density profile determines the [eta] second order shift of the trapped ions as discussed in Appendix 1.

### Ion Orbits

After the density equation has been solved the total potential seen by an ion is computed from  $\Phi_{\text{total}}(\rho) = k_B T \cdot \ln(n(0)/n(\rho))$ . An orbit in this 2-dimensional central force has two constants of motion [9], the angular momentum  $l_z$  around the z axis and the total energy in the  $(\rho, \theta)$  plane  $E_{\text{trans}}$ , i.e., the kinetic plus potential energies. Following the procedures described in appendix 2 an initial position and velocity are generated consistent with the radial density profile for a set linear density  $N/l$ , and the

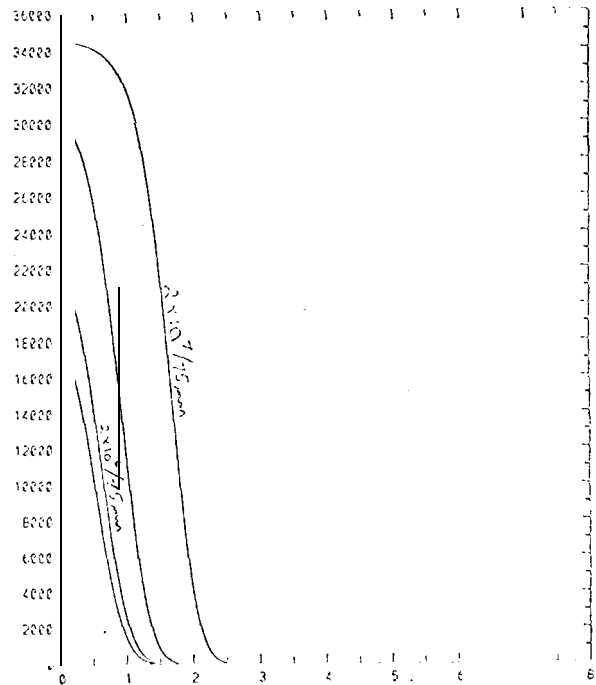


Figure 5: Calculated ion density profiles for 500 K ion temperature at 62 kHz trap secular frequency. The highest density shown is  $2 \times 10^7$  ions in 75 mm length.

Maxwell-Boltzmann velocity distribution at temperature ' $T$ '.  $l_z$  and  $E_{\text{trans}}$  are computed at  $l$  is initial point and the radial turning points of the orbit are found by solving  $E_{\text{trans}} - \Phi_{\text{total}}(\rho) - l_z^2 / 2m\rho^2 = 0$ . The orbits are integrated to the radial turning points to find the angular turning points [9]

$$d\rho = (2(E_{\text{trans}} - \Phi_{\text{total}}(\rho) - l_z^2 / 2m\rho^2) / m)^{1/2} dt$$

$$d\theta = (l_z / m\rho^2) dt.$$

Since the orbits are invariant under reflection about the turning points [9] the complete trajectory is generated by a number of successive reflections. The motion of an ion along the z-axis of the trap is assumed to be a uniform velocity (generated from the velocity distribution as described in Appendix 2) back and forth between the trap ends. For each initial condition a trajectory of duration  $\approx 4$  msec is generated. A time scale common to all the trajectories is generated so that the autocorrelation function at each time step  $\tau_n$  is averaged over the 4,000 to 10,000 trajectories typically employed. This function is then Fourier transformed to give the power spectral density seen by the ensemble of moving atoms.

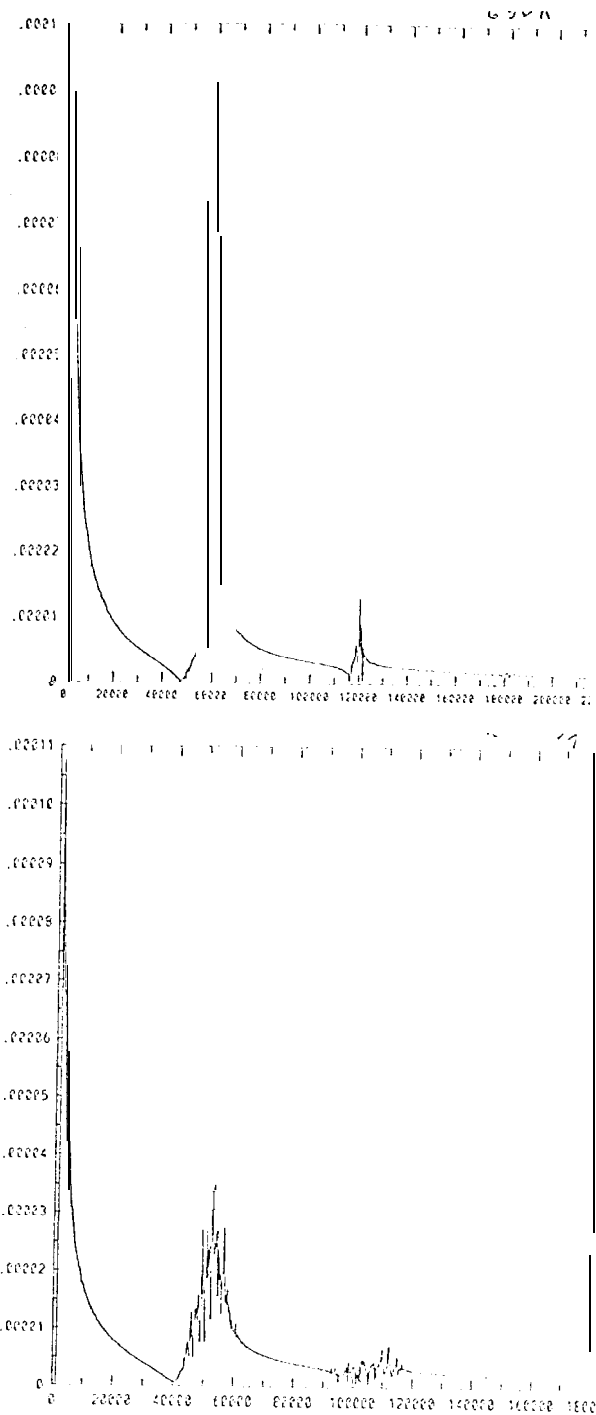


Figure 6: Simulated sideband structure for transverse propagation of 40.5 GHz radiation across ion cloud. The upper curve corresponds to 650 K with  $5 \times 10^5$  ions in 75 mm length. The lower curve at 650 K with  $2.5 \times 10^6$  ions in 75 mm has sidebands shifted in by 10 kHz from the 62 kHz trap secular frequency in agreement with the measured shift of Fig. 4(b).

### Comparison with measured Sideband Frequency

Figure 6 shows the simulated sideband structure for a cloud of ions at 650 K of linear density  $5 \times 10^5$  ions per 75 mm at 62 kHz trap secular frequency. Under these conditions the sidebands are sharp and are slightly displaced inward from the 62 kHz secular frequency. As the linear density is increased to about  $2.5 \times 10^6/75$  mm the sidebands shift inward by about 10 kHz as shown in the measurement of Figure 4(b). The doppler frequency shift under these conditions is  $-4.5 \times 10^{-13}$  from thermal motion and  $-4.3 \times 10^{-13}$  from the micromotion generated by the trapping field. These are the approximate conditions for which the  $1 \text{ Ig}^+$  clock stability of  $7 \times 10^{-14} \tau^{-1/2}$  was obtained [4].

### Conclusions

We have developed a spectroscopic method for measuring temperature, ion number and the resulting 2nd order Doppler shift of the 40.5 GHz clock transition for  $\text{Hg}^+$  ions in a linear ion trap. The ion cloud temperature is obtained from the Doppler broadened width of the 40.5 GHz Zeeman transition when the microwaves are propagated along the axis of the  $1.1^+1^-$ . The ion number is then determined by modelling the frequency of the secular sidebands obtained when the 40.5 GHz radiation propagates across the ion cloud. In clock operation with  $7 \times 10^{-14} \tau^{-1/2}$  stability we have used this method to measure a  $-8.8 \times 10^{-13}$  frequency of offset due to 2nd order Doppler shift at 650 K and linear ion density  $2.5 \times 10^6/75$  mm.

### Appendix 1: Total Second-Order Doppler Shift for fixed T and $N/L$

The resonance frequency,  $f_0$ , of an ion moving with total velocity  $V$  will be shifted by  $\Delta f$  from that of a stationary ion by  $\Delta f/f_0 = -V^2/2c^2$ . For an ion in an rf trap the velocity is the sum of a driven motion  $V_{\text{micro}}$  and a random thermal motion  $V_{\text{th}}$ . The micromotion velocity  $V_{\text{micro}}$  is determined by an ion's position in the trap whereas the magnitude and direction of  $V_{\text{th}}$  is uncorrelated with an ion's position. The average second order dopplershift for an ensemble of ions at temperature  $T$  is

$$-\langle (V_{\text{micro}} + V_{\text{th}})^2 \rangle / 2c^2 = -\langle (V_{\text{micro}}^2 + V_{\text{th}}^2) \rangle / 2c^2$$

because the average over the product  $V_{\text{micro}} \cdot V_{\text{th}}$  vanishes. The two sources can thus be computed separately. Since the average of  $V_{\text{th}}^2$  over the velocity distribution

is  $3k_B T/m$ , the contribution from the thermal motion is  $-3k_B T/2mc^2$ .

The contribution from the micro-motion is the average of  $V_{\text{micro}}^2$  over the density distribution  $n(\rho)$  as determined numerically from eq. (1). The time averaged micro-motion grows with radial distance  $\rho$ ,  $V_{\text{micro}}^2 = \omega^2 \rho^2$  [10] so that

$$\overline{V_{\text{micro}}^2} = \int n(\rho) \rho \omega^2 \rho^2 d\rho / \int n(\rho) \rho d\rho.$$

In the limit of large  $\lambda_D$ , the solution to eq. (1) is  $n(\rho) = n(0) \exp(-\rho^2/4\lambda_D^2)$  and the 2nd doppler from trap field generated ion motion is  $-k_B T/mc^2$ . This is 2/3 of the thermal contribution and stems from the fact that rf or ponderomotive forces provide the trapping in 2 of the 3 spatial dimensions. By contrast, when  $\lambda_D$  is very small compared to the ion cloud radius, the solution to eq. (1) is  $n(\rho) = n_0$  out to the cloud radius  $R_c = ((N/I)/n_0\pi)^{1/2}$ . In this limit, the trap field induced 2nd order doppler shift is  $-(q^2/8\pi\epsilon_0 mc^2)N/I$ .

## Appendix 2: Selection of Initial Positions and Velocities

The selection of the six initial position and velocity coordinates for an ion ensemble at temperature  $T$  with density distribution  $n(\rho)$  is at the heart of the averaging procedure used to compute the autocorrelation function. We follow the technique outlined in references [11,12] and will illustrate selection of the initial radial position coordinate. We compute the probability distribution for an ion's radial position from the computed density profile  $n(\rho)$ . The number of ions found between  $\rho$  and  $\rho + d\rho$  is  $2\pi n(\rho)\rho d\rho$  so that the probability distribution for radial position  $p(\rho)$  is

$$p(\rho) = n(\rho)\rho / \left( \int_0^\infty n(\rho)\rho d\rho \right).$$

A random number,  $\xi$ , is selected in the interval (0,1) with the corresponding radial position  $\rho_\xi$  selected so that  $\xi = \int_0^{\rho_\xi} p(\rho) d\rho$ . The selection frequency of the radial position  $p$  is then in agreement with the distribution  $p(\rho)$ . All six of the initial values are chosen in this manner, the magnitude of the ion velocity from the Maxwell-Boltzmann distribution at temperature  $T$ , the angle of the ion velocity along the trap longitudinal direction ( $z$ -axis) from  $\Theta_\xi = \cos^{-1}(1-2\xi)$ , and so forth. For each of the six initial values an independent

random number  $\xi$  is chosen so that there is no correlation. A representative histogram of initial velocity components along the  $z$  direction generated from the speed and direction sampling is shown in Figure A(1) for an ion temperature of 500 K.

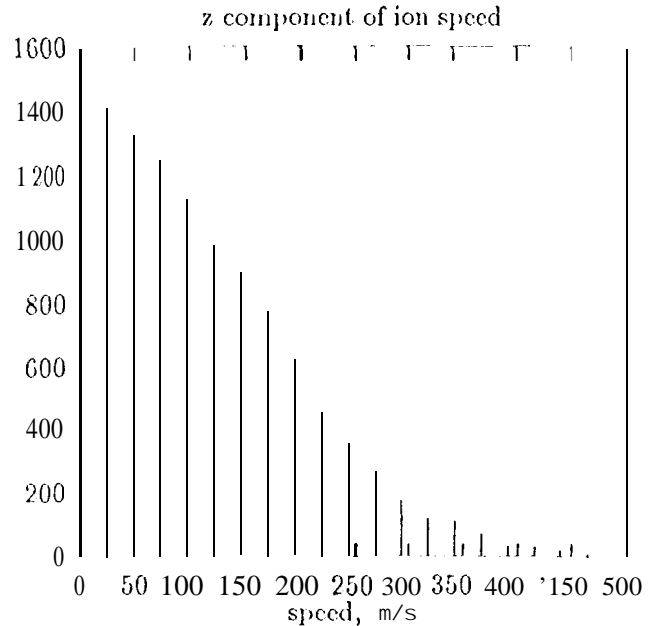


Figure A(1): The generated distribution of the  $z$  component of ion velocities. This histogram is created from two independently generated distributions- the Maxwell distribution of ion speeds and the velocity direction angle distribution with respect to the trap longitudinal axis.

## References

- [1] J. D. Prestage, R. L. Tjoelker, R. J. Wang, G. J. Dick, and L. Maleki, " $^{199}\text{Tl}^+$  Trapped Ion Standard with the Superconducting Cavity Maser Oscillator," *IEEE Trans. Instr. Meas.*, vol. 42, No. 2, April 1993.
- [2] L. S. Cutler, R. P. Giffard, P. J. Wheeler, and G. M. R. Winkler, "Initial Operational Experience with a Mercury 1011 Storage Frequency Standard," *Proc 41st Ann. Symp. Freq. Control*, pp. 12-19, 1987.
- [3] L. S. Cutler, R. P. Giffard, and M. D. McGuire, "Thermalization of  $^{199}\text{Tl}$  Ion Macro-motion by a Light Background Gas in an RF Quadrupole Trap," *Appl. Phys. B* 36, pp. 137-142, 1985.

[4] R. L. Tjoelker, J. D. Prestage, G. J. Dick, and L. Maleki, "Long Term Stability of  $\text{Hg}^+$  Trapped Ion Frequency Standards," Proc. 47th Ann. Symp. Freq. Control, June 1993.

[5] R. H. Dicke, "The Effect of Collisions upon the Doppler Width of Spectral Lines," Phys. Rev. 89, pp. 472-473, Jan. 1953.

[6] A. Corney, Atomic and Laser Spectroscopy. Oxford: Clarendon Press, 1977, ch. 8, pp. 248-249.

[7] L. S. Cutler, C. A. Flory, R. P. Giffard, and M. D. McGuire, "Doppler Effects due to Thermal Macromotion of Ions in an RF Quadrupole Trap," Appl. Phys. B 39, pp. 251-259, 1986;

C. Meis, M. Desaintfuscién, and M. Jardino, "Analytical Calculation of the Space Charge Potential and the Temperature of Stored Ions in an rf Quadrupole Trap," Appl. Phys. B 45, pp. 59-64, 1988.

[8] G. R. Janik, J. D. Prestage, and L. Maleki, "Simple Analytic Potentials for Linear Ion Traps," J. Appl. Phys. 67, pp. 6050-6055, Jan. 1990.

[9] H. Goldstein, Classical Mechanics. Reading: Addison-Wesley, 1950, ch. 3, pp. 59-63.

[10] J. D. Prestage, G. J. Dick, and L. Maleki, "New Ion Trap for Frequency Standard Applications," J. Appl. Phys. 66(3), pp. 1013-1017, Aug. 1989.

[11] P. K. MacKeown and D. J. Newman, Computational Techniques in Physics. Bristol: Adam Hilger, 1987, ch. 7, pp. 141-145.

[12] S. E. Koonin, Computational Physics. Menlo Park: Benjamin/Cummings, 1986, ch. 8, pp. 191-195.